

Computer Simulation of Phase Decomposition in Fe-Cr-Co Alloy Based on the Phase-Field Method

Toshiyuki Koyama and Hidehiro Onodera

Computational Materials Science Center
Independent Administrative Institution National Institute for Materials Science
1-2-1 Sengen, Tsukuba, Ibaraki, JAPAN 305-0047
Tel : +81-298-59-2635, Fax : +81-298-59-2601,
E-mail : KOYAMA.Toshiyuki@nims.go.jp

The phase-field method has recently been developed as a powerful tool to simulate and predict the complex microstructure developments in many fields of materials science. In this study, the phase decomposition during isothermal aging of Fe-Cr-Co ternary alloy under an external magnetic field is simulated based on the phase-field method. Since the Gibbs energy function that is available from the thermodynamic CALPHAD database of the equilibrium phase diagram is employed in this simulation, the present calculation provides the quantitative microstructure changes directly linked to the phase diagram. The simulated microstructure demonstrates that the lamella shaped microstructure elongated along the external magnetic field is evolved with progress of aging. The morphological and temporal developments of the simulated microstructures show in good agreement with the experimental results that have been observed in this alloy system.

Keywords: phase-field method, phase transformation, phase decomposition, spinodal decomposition, pattern formation, diffusion equation, non-linear

1. INTRODUCTION

Since the factors that influence microstructure formation are extensive (e.g., alloy composition, heat treatment condition, etc.), quite a lot of experimental trial-and-error is often necessary when searching for the best combination of desired microstructure and material properties, even when the basic mechanism of microstructure formation is understood. During the last decade, the phase-field method has emerged across many fields in materials science as a powerful tool to simulate and predict complex microstructure evolution⁽¹⁻⁴⁾. Since phase-field methodology can model complex microstructure changes quantitatively, it is possible to search for the most desirable microstructure by using this method as a design simulation, i.e., through computer trial-and-error testing. In order to establish this methodology, first of all, quantitative modeling of complex microstructure changes using the phase-field method is required.

The objective of this study is to model the spinodal decomposition and the microstructure evolution in Fe-Cr-Co magnetic alloy under external magnetic field. In order to simulate the phase decomposition consistent with the Fe-Cr-Co ternary phase diagram, we employed the Gibbs energy function that has been determined through the CALPHAD method⁽⁵⁾.

2. CALCULATION METHOD

In this study, we considered a three-dimensional system, but the microstructure morphology of the cross section perpendicular to the [100] direction was assumed congruent. Therefore, the present calculation is a

two-dimensional simulation on the (100) plane, essentially.

2.1 Total free energy of microstructure

In order to simulate the microstructure changes quantitatively, the precise evaluation of total free energy of microstructure is required. The total free energy of the inhomogeneous system is expressed as

$$G_{sys} = \int_V \left[G_c^\alpha \{c_i(\mathbf{r}, t), T\} + \frac{1}{2} \kappa_c \sum_{i=1}^3 \{\nabla c_i(\mathbf{r}, t)\}^2 \right] d\mathbf{r} \quad (1) \\ + E_{str}(t) + E_{mag}(t, T) ,$$

where G_c^α is the Gibbs energy density, T is temperature. E_{str} and E_{mag} are the elastic strain energy and the magnetic energy, respectively. The second term in [] is the composition gradient energy where κ_c is composition gradient energy coefficient which is assumed constant in this study. $c_i(\mathbf{r}, t)$ is the local composition of element i at position \mathbf{r} and time t in the microstructure. The subscript $i = 1, 2, \text{ and } 3$ means Fe, Cr, and Co, respectively.

The Gibbs energy of α (bcc) phase in Fe-Cr-Co system with magnetic contribution is described by the sub-regular solution approximation⁽⁵⁾

$$G_c^\alpha(c_i, T) = \sum_{i=1}^3 G_i^\alpha c_i + RT \sum_{i=1}^3 c_i \ln c_i \quad (2) \\ + {}^E G^\alpha + {}^{mg} G^\alpha ,$$

$${}^E G^\alpha \equiv L_{1,2}^\alpha c_1 c_2 + L_{1,3}^\alpha c_1 c_3 + L_{2,3}^\alpha c_2 c_3$$

$${}^{mg} G^\alpha \equiv RT \ln(\beta^\alpha + 1) f(\tau), \quad \tau \equiv T / T_C^\alpha$$

where ${}^o G_i^\alpha$ is the Gibbs energy of pure element i in the case of the crystal structure is bcc. R is gas constant. ${}^E G^\alpha$ is the excess free energy corresponding the heat of mixing, and ${}^{mg} G^\alpha$ is the magnetic contribution to the Gibbs energy. $f(\tau)$ is defined⁽⁵⁾ as a function of $\tau (\equiv T / T_C^\alpha)$. The interaction parameter $L_{i,j}^\alpha$, the Curie temperature T_C^α , and the atomic magnetic moment β^α are available from the CALPHAD database⁽⁵⁾, respectively, as a function of composition and temperature. We used following data⁽⁶⁾:

$$L_{1,2}^\alpha = 20500 - 9.68T$$

$$L_{1,3}^\alpha = -23669 + 103.9627T - 12.7886T \ln T$$

$$L_{2,3}^\alpha = (24357 - 19.797T) - 2010(c_3 - c_2), \quad (\text{J/mol})$$

$$T_C^\alpha = 1043c_1 - 311.5c_2 + 1450c_3 + \{1650 + 550(c_2 - c_1)\}c_1 c_2 + 590c_1 c_3, \quad (\text{K})$$

$$\beta^\alpha = 2.22c_1 - 0.01c_2 + 1.35c_3 - 0.85c_1 c_2 + \{2.4127 + 0.2418(c_3 - c_1)\}c_1 c_3.$$

(Bohr magneton unit)

The crystal structure considered in this simulation is bcc only, so that we adopted ${}^o G_1^\alpha = {}^o G_2^\alpha = {}^o G_3^\alpha = 0$ as the reference energy level for the Gibbs energy.

The elastic strain energy^(7,8), E_{str} , is represented as

$$E_{str} = \frac{1}{2} \int C_{ijkl} \varepsilon_{ij}^{el}(\mathbf{r}, t) \varepsilon_{kl}^{el}(\mathbf{r}, t) d\mathbf{r}, \quad (3)$$

$$\varepsilon_{ij}^{el}(\mathbf{r}, t) \equiv \varepsilon_{ij}^c(\mathbf{r}, t) - \varepsilon_{ij}^0(\mathbf{r}, t)$$

where $\varepsilon_{ij}^{el}(\mathbf{r}, t)$ is elastic strain^(7,8) and C_{ijkl} is the elastic constant. The stress free strain, $\varepsilon_{ij}^0(\mathbf{r}, t)$, is expressed as

$$\varepsilon_{ij}^0(\mathbf{r}, t) = \begin{bmatrix} \varepsilon_2 \{c_2(\mathbf{r}, t) - c_2^0\} \\ + \varepsilon_3 \{c_3(\mathbf{r}, t) - c_3^0\} \end{bmatrix} \delta_{ij}, \quad (4)$$

where ε_i is the lattice mismatch, c_i^0 is the average composition of element i , and δ_{ij} is Kronecker's delta.

The constrained strain, $\varepsilon_{ij}^c(\mathbf{r}, t)$, is given as

$$\varepsilon_{kl}^c(\mathbf{r}, t) = \int_{\mathbf{k}} \left[\Omega_{ik}(\mathbf{n}) n_j n_l C_{ijpq} \delta_{pq} \left\{ \varepsilon_2 \hat{c}_2(\mathbf{k}, t) + \varepsilon_3 \hat{c}_3(\mathbf{k}, t) \right\} \right] \times \exp(i\mathbf{k} \cdot \mathbf{r}) \frac{d\mathbf{k}}{(2\pi)^3}, \quad (5)$$

where $\Omega_{ik}(\mathbf{n})$ is the inverse matrix of

$\Omega_{ik}^{-1}(\mathbf{n}) \equiv C_{ijkl} n_j n_l$. \mathbf{k} is a reciprocal space vector and $\mathbf{n} \equiv \mathbf{k} / |\mathbf{k}|$ is unit vector along \mathbf{k} direction. $\hat{c}_i(\mathbf{k}, t)$ is the Fourier transform of $c_i(\mathbf{r}, t)$ field.

In this study, we considered the demagnetizing energy⁽⁹⁾, E_d , as the magnetic energy E_{mag} which influence the phase decomposition. E_d is a dipole-dipole interaction energy between magnetic moments, and expressed as

$$E_d = \frac{1}{2\mu_0} \sum_{i=2}^3 \sum_{j=2}^3 \int \int \left[\left(\frac{\partial M_S}{\partial c_i} \right)_{c_i, c_j} \{c_i(\mathbf{r}) - c_i^0\} \right] \times m_k(\mathbf{r}) W_{kl}(\mathbf{r} - \mathbf{r}') m_l(\mathbf{r}') \left[\left(\frac{\partial M_S}{\partial c_j} \right)_{c_i, c_j} \{c_j(\mathbf{r}') - c_j^0\} \right] d\mathbf{r} d\mathbf{r}' \quad (6)$$

$$W_{ij}(\mathbf{r} - \mathbf{r}') \equiv \frac{1}{4\pi} \left(\frac{\delta_{ij}}{|\mathbf{r} - \mathbf{r}'|^3} - \frac{3(r_i - r'_i)(r_j - r'_j)}{|\mathbf{r} - \mathbf{r}'|^5} \right).$$

μ_0 is permeability of vacuum. M_S is the absolute value of magnetization moment vector which depends on the composition and temperature. $\mathbf{m}(\mathbf{r})$ is the normalized magnetization moment ($|\mathbf{m}(\mathbf{r})| = 1$). It is known that the intensity of magnetization, $I(\tau)$, which is normalized by saturation magnetization, is expressed theoretically by the Brillouin function⁽¹⁰⁾. Then we approximate the function to analytical form as follows⁽⁵⁾:

$$I(\tau) = 1 - \frac{1}{7}(5\tau^4 + 2\tau^{20}), \quad (\tau \leq 0.9)$$

$$I(\tau) = 2^{-2+10(\tau-1)}, \quad (\tau > 0.9)$$

Using the following functions, $I(\tau)$, T_C^α and β^α , we obtain the magnetization moment $\mathbf{M}(\mathbf{r}, t)$ as

$$\mathbf{M}(\mathbf{r}, t) = M_S(c_i, \tau) \mathbf{m}(\mathbf{r}) \quad (7)$$

$$M_S(c_i, \tau) \equiv \beta_{Bohr}^0 \beta^\alpha I(\tau), \quad (\text{T}),$$

where β_{Bohr}^0 is the Bohr magneton. It is quite important to note that $M_S(c_i, \tau)$ is represented as a function of composition and temperature because β^α and τ have composition and temperature dependence (τ is a function of T_C^α). Therefore, we can calculate $\partial M_S / \partial c_i$ in eq.(6) analytically based on eq.(7).

2.2 Phase-field method

The phase-field method is the computer simulation method to calculate the dynamics of temporal microstructure changes by solving the continuum non-linear evolution equations for the conserved and non-conserved order parameters⁽¹⁻⁴⁾. In this work, since we consider the composition field only, the phase-field method used here is the same as that of the computer simulation by the Cahn-Hilliard non-linear diffusion

equation⁽¹¹⁾. The evolution equations governing the phase decomposition in Fe-Cr-Co ternary system are expressed by

$$\begin{aligned} \frac{\partial c_2}{\partial t} &= \nabla \cdot \left(L_{22} \nabla \frac{\delta G_{sys}}{\delta c_2} + L_{23} \nabla \frac{\delta G_{sys}}{\delta c_3} \right) \\ \frac{\partial c_3}{\partial t} &= \nabla \cdot \left(L_{32} \nabla \frac{\delta G_{sys}}{\delta c_2} + L_{33} \nabla \frac{\delta G_{sys}}{\delta c_3} \right), \end{aligned} \quad (8)$$

where the Onsager coefficients, L_{ij} , are determined using the self diffusion coefficient D_i^* as

$$L_{22} = [c_1 c_2 D_1^* + (1 - c_2)^2 D_2^* + c_2 c_3 D_3^*] \frac{c_2}{RT}$$

$$L_{33} = [c_1 c_3 D_1^* + c_2 c_3 D_2^* + (1 - c_3)^2 D_3^*] \frac{c_3}{RT}$$

$$L_{23} = L_{32} = [c_1 D_1^* - (1 - c_2) D_2^* - (1 - c_3) D_3^*] \frac{c_2 c_3}{RT}.$$

Numerical values used in this simulation are summarized in Table I.

Table I Numerical values used for the calculation

Temperature, T / K	873, 913
Composition gradient energy coefficient, $\kappa_s / J \cdot m^{-2} \cdot mol^{-1}$	1.0×10^{-14}
Lattice mismatch ⁽¹²⁾ , ε_i	$\varepsilon_2 = 6.1 \times 10^{-3}$ $\varepsilon_3 = -7.1 \times 10^{-3}$
Elastic coefficients ⁽¹²⁾ of element X, C_{ij}^X / GPa (Elastic coefficients for bcc Co is assumed as $C_{ij}^{Co} = C_{ij}^{Fe}$.)	$C_{11}^{Fe} = 233.1$ $C_{12}^{Fe} = 135.44$ $C_{44}^{Fe} = 117.83$ $C_{11}^{Cr} = 350$ $C_{12}^{Cr} = 67.8$ $C_{44}^{Cr} = 100.8$
Self diffusion coefficient ⁽¹²⁾ of component i , $D_i^* = D_i^0 \exp(-Q_i / RT)$, $D_i^0 / m^2 \cdot s^{-1}$, $Q_i / kJ \cdot mol^{-1}$ (Self diffusion coefficient for bcc Co is assumed as $D_3^* = D_1^*$.)	$D_1^0 = 1.0 \times 10^{-4}$ $Q_1 = 294$ $D_2^0 = 2.0 \times 10^{-5}$ $Q_2 = 308$
Calculation area, $L \times L / nm^2$	160×160

Figure 1(a) and (b) show the metastable phase diagrams of bcc phase in the Fe-Cr-Co ternary alloy system, calculated using CALPHAD database⁽⁶⁾, at 873K and 913K, respectively. It is noted that the ($\alpha_1 + \alpha_2$) two phases region of Fe-Cr binary phase diagram is widely extended with increasing Co content. Average composition of the alloy used in this simulation is denoted by solid circle. The thin straight lines inside the two phases region are the calculated tie lines.

3. SIMULATION RESULTS AND DISCUSSIONS

3.1 Isothermal phase decomposition

Figure 2 shows the two-dimensional simulation result for the phase decomposition of α -bcc phase at 873K. The average composition of the alloy is Fe-40at%Cr-

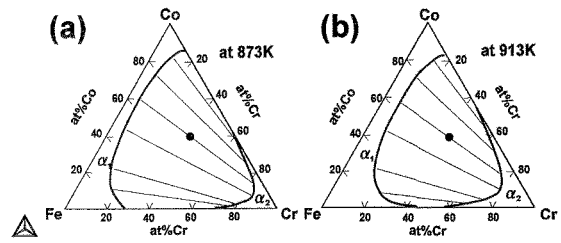


Fig.1 Calculated phase diagrams of Fe-Cr-Co system.

40at%Co. The temporal microstructure change during isothermal phase decomposition is demonstrated from the top layer to bottom in Fig.2. Three columns of Fig.2 correspond to composition fields of Fe, Cr, and Co, respectively. The local composition is represented by gray scale, and darkness means the high concentration of corresponding element. Numerical values in the figure indicate the dimensionless normalized aging time. Figure 2(a) is the initial state of the supersaturated solid solution with small composition fluctuation that is imposed as Gaussian noise. At the initial stage of spinodal decomposition, the Cr-rich α_2 phase is nucleated in α_1 matrix (see Fig.2(b)). With progress of aging, as seen from Fig.2(c) to (d), the precipitates coarsening occurs by the mechanism of Ostwald ripening.

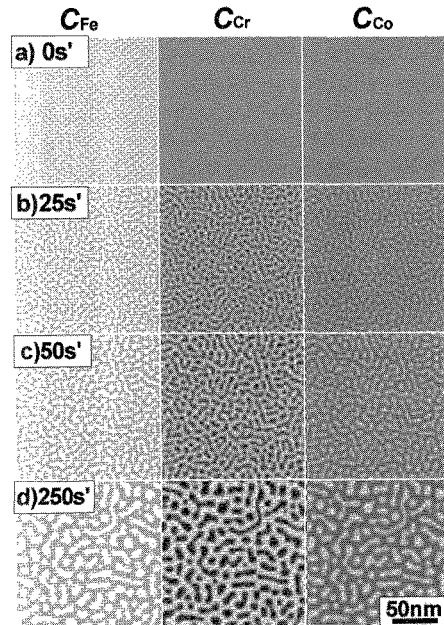


Fig.2 Calculation of phase decomposition in Fe-40at%Cr-40at%Co alloy at 873K.

Figure 3 is the simulation at 913K and the other calculation condition is the same as that of Fig.2. It is interesting that the initial nucleation phase is not α_2 phase but α_1 phase (Fig.3(a)). During aging, the volume fraction of α_1 phase increases, then the α_1 precipitates connect each other (Fig.3(b)), finally, α_1 phase becomes matrix (Fig.3(c)).

The phase decomposition under external magnetic field applied along the horizontal direction is demonstrated in Fig.4. The calculation condition except for the magnetic field is same as Fig.3. We assumed the

magnetic field is strong enough to align all magnetic spin in the microstructure to the direction of external magnetic field. It is clearly recognized that the lamellar shaped microstructure elongated along the external magnetic field appears.

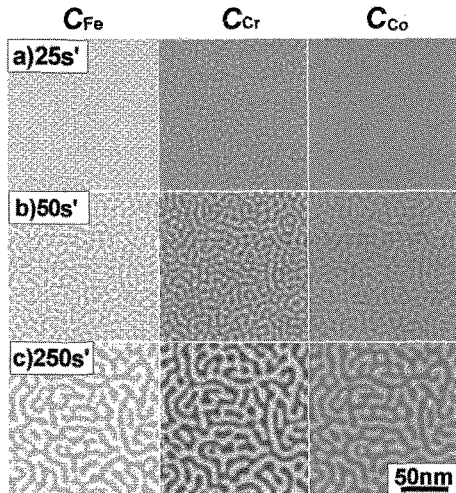


Fig.3 Calculation of phase decomposition in Fe-40at%Cr-40at%Co alloy at 913K.

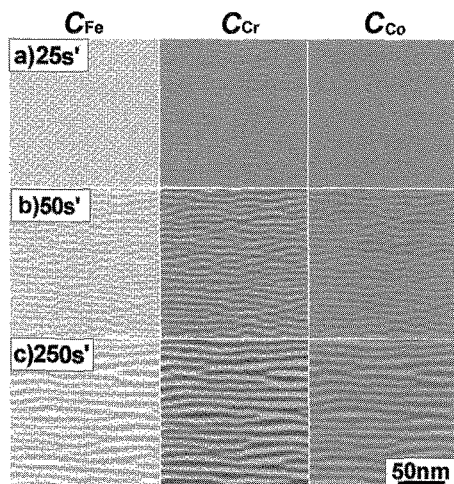


Fig.4 Calculation of phase decomposition in Fe-40at%Cr-40at%Co alloy at 913K under external magnetic field.

Figure 5 shows the TEM bright field images of microstructure in Fe-33at%Cr-22at%Co alloy, investigated by Okada *et al.*⁽¹³⁾; (a) aged at 873K for 360ks, (b) at 913K for 1.2ks, and (c) at 913K in magnetic field of 2kOe for 10.8ks, respectively. White part in micrographs is Fe-rich region.

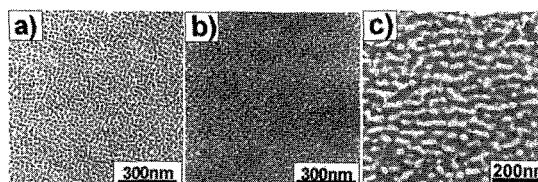


Fig.5 TEM bright field images of Fe-33at%Cr- 22at%Co alloy⁽¹³⁾; (a) aged at 873K for 360ks, (b) at 913K for 1.2ks, and (c) at 913K in magnetic field of 2kOe for 10.8ks, respectively.

The average alloy composition used in calculation is slightly different from the experiment, but the morphological features of the simulated microstructures in Figs.2-4 show in good agreement with the experimental results^(13,14).

4. CONCLUSIONS

We attempted to model the microstructure changes during isothermal phase decomposition in Fe-Cr-Co magnetic alloy using the phase-field method, where the Gibbs energy function is directory linked to the CALPHAD database. The results obtained are as follows: (1) The simulated microstructure changes agree well with the experimental results that have been observed in this alloy system. (2) Whether α_1 phase becomes the droplet shaped precipitate at the initial stage of spinodal decomposition depends on the aging temperature. (3) The external magnetic field effects on the microstructure formation, and the morphology of microstructure becomes lamellar shape that is elongated along the external magnetic field. (4) Phase-field simulation linked to the CALPHAD approach will be quite useful to design the microstructure in real alloy systems. Especially, the CALPHAD database is applicable not only for the Gibbs energy estimation but also the magnetic energy evaluation.

ACKNOWLEDGEMENTS

This work was partly supported by a NEDO International Joint Research Grant on "Structuring Knowledge, Science and Technology for Nano Material Processing", and also supported by the Special Coordination Funds for Promoting Science and Technology on "Nanohetero Metallic Materials" and NAREGI Nanoscience PJ from the Ministry of Education, Culture, Sport, Science and Technology, Japan.

REFERENCES

- [1] T. Koyama: *Materia Japan* (Bull. of the Japan Inst. Metals), **42**, 397-404 (2003).
- [2] L-Q.Chen: *Annu.Rev.Mater.Res.*, **32**, 113-40 (2002).
- [3] W.J.Boettinger, J.A.Warren, C.Beckermann, and A.Karma: *Annu. Rev. Mater. Res.*, **32**, 163-94 (2002).
- [4] M.Ode, S.G.Kim and T.Suzuki: *ISIJ Int.*, **41**, 1076-82 (2001).
- [5] N.Saunders and A.P.Miodownik : "CALPHAD", Pergamon, (1998).
- [6] "Thermo-Calc (ver.M)", Thermo Calc software AB.
- [7] A.G.Khachaturyan: "Theory of Structural Transformations in Solids", (Wiley and Sons, New York, 1983) pp.198-212.
- [8] T.Mura; "Micromechanics of Defects in Solids (2nd Rev. ed.), Kluwer Academic, (1991), pp.204-218.
- [9] J.W.Cahn: *J App.Phys.*, **34**, 3581-86 (1963).
- [10] S.Chikazumi: "Physics of Ferromagnetism (2nd ed.)", Oxford, (1997).
- [11] J.E.Hilliard: "Phase Transformation", ed. by H.I.Aaronson, ASM, Metals Park, Ohio, (1970), pp.497-560.
- [12] "Metals data book", Japan Institute of Metals(ed.), Maruzen, (1993).
- [13] M.Okada,G.Thomas,M.Homma and H.Kaneko: *IEEE Trans. Mag.*, **14**, 245-52 (1978).
- [14] T.Minowa, M.Okada and M.Homma: *IEEE Trans. Mag.*, **16**, 529-33 (1980).